



Transworld Research Network
37/661 (2), Fort P.O.
Trivandrum-695 023
Kerala, India

Liquid Crystalline Organic Compounds and Polymers as Materials of the XXI Century:
From Synthesis to Applications, 2011: 153-189 ISBN: 978-81-7895-496-7
Editor: Agnieszka Iwan

6. New strategy in development of liquid crystal photoaligning materials with reactive C=C bonds

Lyudmyla Vretik¹, Oleg Yaroshchuk², Valentyna Zagnii¹, Vasyl Kyrychenko¹
and Volodymyr Syromyatnikov¹

¹*Department of Macromolecular Chemistry, Kyiv National Taras Shevchenko University
Volodymyrs'ka St. 60, 01033 Kyiv, Ukraine;* ²*Department of Physics of Crystals
Institute of Physics, NASU, prospect Nauky 46, 03680 Kyiv, Ukraine*

Abstract. We review our recent approaches in development of polymers for liquid crystal (LC) photoalignment. The designed polymers contain side photosensitive chains with aromatic core and terminal tetrahydrophthalic/maleimide/methacrylamide groups. Under the action of actinic UV light these materials undergo Fries rearrangement and crosslinking due to photoaddition/photopolymerization that in case of polarized light illumination results in highly efficient LC alignment. It is shown that Fries rearrangement causes pronounced photoalignment effect, while the photocrosslinking determines the alignment stability.

Introduction

Liquid crystal (LC) alignment is one of the key issues of LC displays and LC photonic devices in general. For operation of these devices in a certain

Correspondence/Reprint request: Dr. Oleg Yaroshchuk, Department of Physics of Crystals, Institute of Physics, NASU, prospect Nauki, 46, 03680 Kyiv, Ukraine. E-mail: o.yaroshchuk@gmail.com

mode, LC alignment should be thoroughly optimized; it should demonstrate adjusted pretilt angle and anchoring energy, high macroscopic and microscopic uniformity, and outstanding stability. Quite often, for operation in multidomain modes, the alignment parameter should be spatially modulated.

LC alignment is commonly achieved by a proper treatment of substrates confining LC layer. This treatment provides surface anisotropy of the substrates and, as result, anisotropic LC-surface interaction. Due to long-range orientational interaction in the liquid crystal phase, LC alignment given by the surface extends into the liquid crystal bulk on a macroscopic scale. It allows one to obtain liquid “single-crystals” in cells with a thickness varied from a few to hundreds of microns.

The conventional treatment procedure of the aligning substrates is rubbing. The substrates unidirectionally rubbed provide tilted LC alignment with a pretilt angle at the substrate mainly determined by the chemical composition of the aligning material. This procedure is quite reliable, provides strong anchoring and reproducible pretilt angle, as well as high thermal stability of LC alignment. At the same time, the rubbing method has number of intrinsic drawbacks, which quite often seriously hamper its application in an industry. The major problem is a direct mechanical contact with the aligning surface resulting in formation of scratches and large static charges causing surface dusting, cross-track shorts, and failure of thin film transistors [1].

The inherent problems of rubbing alignment technique stimulated development of alternative alignment methods capable to eliminate the rubbing problems and compete with it in industry. Among these alternative methods, the photoalignment technique [2-5] shows especial promise, because of very favorable set of properties. In contrast to rubbing, this technique provides soft treatment of the aligning surfaces. Avoiding mechanical contact with the substrate, it minimizes mechanical damage and electric charging, provides excellent alignment uniformity, and an easy way for controlling alignment parameters. It is irreplaceable in a number of new LC devices, in which the LC alignment should be induced in closed volumes, on non-flat surfaces, and on the surfaces of microscopic scale used, for example, in optical communication devices.

However, having these advantages, photoalignment technique suffers from other problems such as insufficient alignment stability, relatively weak anchoring, and pronounced image sticking. Despite some new approaches, such as use of deep UV irradiation [6], optical “rubbing” [7], and passivation of photoaligning layers with the thin layers of reactive mesogens [8], the

main efforts to improve the alignment properties are focused on finding new materials suiting better for application in photoalignment.

This paper describes some advances in this direction. Although it is mainly based on results of our researches, it also gives a brief review of other recent achievements in this field. The paper is organized as follows. At first we give brief introductory section, which covers principles and challenges of photoalignment technique and the idea of the present research. Section 2 gives the experimental details, and sections 3-6, the main sections of this work, describe newly synthesized polymers and their photoaligning characteristics. Finally, section 7 presents concluding remarks.

1. Background information

Despite of nice books and reviews on photoalignment [1, 9-11], we decided to give concise introduction to this phenomenon with making focus on the challenges of the state-of-the-art photoalignment materials and modern trends in their improvement. Also, we give minimal information about aligning parameters discussed in the next sections.

1.1. LC alignment characterization

Usually, preferable direction of LC alignment (LC director, \mathbf{d}) near the aligning substrate, \mathbf{d}_s , is characterized by azimuthal angle φ and polar angle θ , usually called pretilt angle (Fig. 1). Depending on value of pretilt angle, planar ($\theta = 0$), homeotropic ($\theta = 90^\circ$) and tilted ($0^\circ < \theta < 90^\circ$) alignment is distinguished.

The alignment direction \mathbf{d}_s is determined by a balance of anchoring and elastic forces, as well as external forces applied to the LC layer. For this reason, \mathbf{d}_s does not necessarily coincide with the direction set by the alignment process (easy axis direction, \mathbf{l}). The deviation of \mathbf{d}_s from \mathbf{l} determines degree of orientational anchoring of LC with the aligning substrate. If this deviation is not so strong, orientational part of surface free energy of LC, F_s , can be presented in the Rapini-Papoular form

$$F_s = \frac{1}{2}W(\vec{n}\vec{l}), \quad (1)$$

where W is a parameter with dimension of energy. This parameter is called anchoring coefficient or, simply, anchoring energy. It can be interpreted as energy per unit area needed to deviate LC director from the easy direction \mathbf{l} .

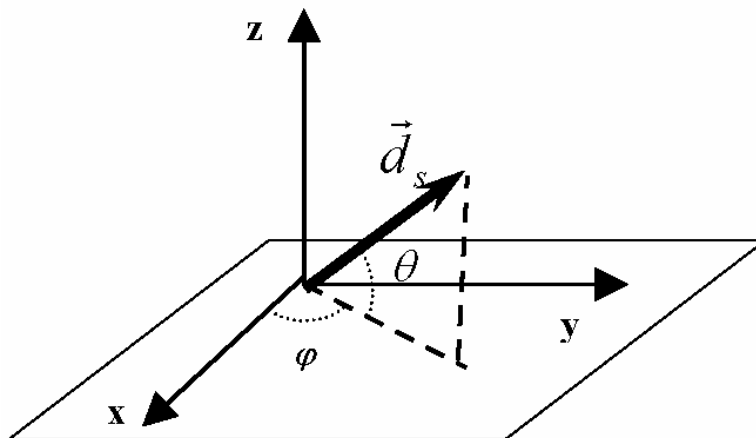


Figure 1. Characterization of LC alignment near the aligning surface.

It can also be considered as a surface elastic constant, material constant depending on the properties of aligning surface and LC. Considering the in-plane and the out-of-plane deviation of \vec{d} (with regard to the plane of aligning substrate) one can select azimuthal and polar anchoring coefficients, W_a and W_p . These parameters determine director field in the cell, electro- and magneto-optical response, anchoring transitions and many other effects.

1.2. Photoalignment procedure

Film of photoaligning material is exposed to light, which excites photochemical transformations and, in this way, generates surface anisotropy in the film. Commonly, the exciting light is linearly polarized (Fig. 2a), but LC photoalignment with unpolarized light is also described [12,13]. In the latter case, the induced anisotropy is caused by oblique exposure (Fig. 2b). In the majority of photoaligning materials easy axis of LC alignment is induced in the direction perpendicular to the light polarization. However, there are groups of materials providing LC alignment in the direction of light polarization, or in both these directions [14-17].

The conventional polarized light procedure (Fig. 2a) does not set direction of LC inclination. As a result, the induced alignment shows twofold degeneration of pretilt angle. To set the inclination direction unambiguously, the polarized light exposure (Fig. 2a) is usually combined with the oblique illumination with unpolarized light (Fig. 2b) or polarized light with perpendicular direction of polarization [18,19]. These two stages can be realized simultaneously by employing oblique illumination with partially polarized light. Alternatively to the oblique exposure, the pretilt angle direction can be unambiguously set in so named photorubbing process recently

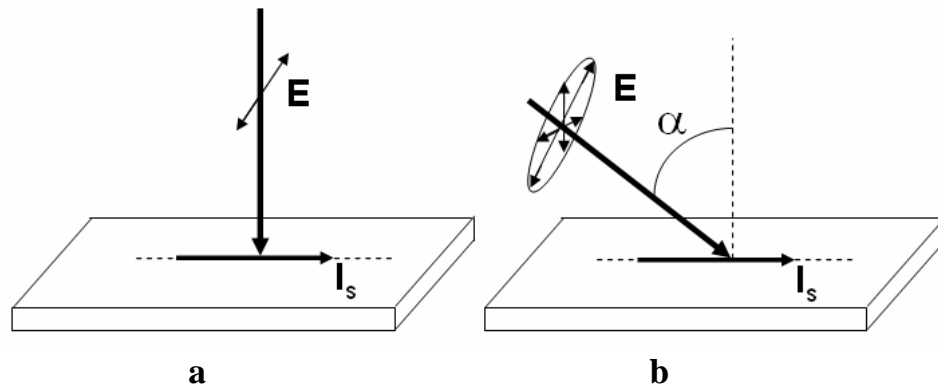


Figure 2. Exposure schemes used in photoalignment process. Cases (a) and (b) correspond to polarized and unpolarized illumination, respectively, I_s marks in-plane projection of light induced easy axis.

developed [7]. In this process, the photoalignment layer is unidirectionally scanned during illumination with periodically modulated light resulting in the LC inclination towards the scanning direction.

Illumination through photo-masks is commonly used to realize patterned alignment. The amount of mask illumination processes can be reduced by using materials allowing optical rewriting.

1.3. Photoalignment mechanisms

Illumination with exciting light stimulates photochemical transformations of photosensitive fragments of photoalignment materials. Usually, these absorbing parts have elongated shape and are characterized by anisotropy of absorption. Due to these properties, illumination with polarized light results in transformation of initially isotropic orientational distribution of photosensitive fragments into the anisotropic one. Depending on the nature of photochemical transformations, this occurs by angular photoselection (angular hole burning) or angular redistribution (molecular photo-reorientation) [20-22]. The non-photosensitive units of photoalignment materials can also be involved in this ordering process [23, 24]. As result, the exposed film becomes anisotropic (Weigert effect [25]). The orientational order induced in the bulk of photoalignment film and on its surface well correlate, but this correlation can be distorted by the processes of self-organization (self-assembly) occurring on the surface of the photoalignment films [26,27].

The LC molecules adjacent to the orientationally ordered photoalignment film reproduce to certain extent this order due to anisotropic interaction with

the molecules or anisotropic fragments from the surface of this film [28]. The van der Waals, dipole-dipole, π - π stacking, hydrogen bonding or steric interaction may dominate depending of molecular structure of LC and photoaligning material, as well as the nature of their self-organization. The processes of anisotropic LC adsorption/desorption coupled with surface memory may also be important in the alignment mechanism. Finally, some authors support the view that the alignment direction is determined mainly by the morphological anisotropy, while the magnitude of the anchoring energy depends on the LC and aligning material interaction [29,30].

1.4. Photoalignment materials

The photoaligning materials are usually classified according to the prevailing photochemistry. Initially, the photoalignment phenomenon was observed for the materials with photosensitive species undergoing *trans-cis* photoisomerization (Fig. 3a). This group primarily includes azocompounds: chemically [2] and physically [31] adsorbed azodyes, azodye blends and azopolymers [5]. The second group comprises materials susceptible to photodestruction, such as photooxidation, chain scission, etc. (Fig. 3b). The examples of these materials are photosensitive polyimides [32], polysilanes [33] and polystyrene [34]. Third, the most studied group includes materials undergoing photo-crosslinking of cycloaddition type. The materials containing cinnamate [3,4], coumarin [35] and chalconyl [36] chromophore undergo [2+2] cycloaddition (Fig, 3c). The [4+4] cycloaddition reaction is typical for anthracenyl chromophore [37] (Fig. 3d). These photocrosslinkable moieties can be physically deposited or grafted to the substrate, covalently linked to polymer backbones or blended in polymers.

Each of these types of materials has its advantages and disadvantages. The azo compounds usually give excellent LC alignment low exposure dose, which can be less than 0.05 J/cm^2 . However, this alignment is not sufficiently stable against heat and light, because of reversible photochemistry and orientational disordering of azo fragments. The thermal stability of the photoalignment is essentially higher for sulfuric azodyes, apparently due to strong adsorption of the molecules on the substrate. However, the photostability of these samples is not sufficient. The photodestructive polyimides commonly require high exposure dose (more than 10 J/cm^2). This photochemical process creates net surface charge, which causes enhanced image sticking and display flicker. Moreover, thermal stability of photoalignment is insufficient, because the photodestructed fragments relax under annealing at high temperature.

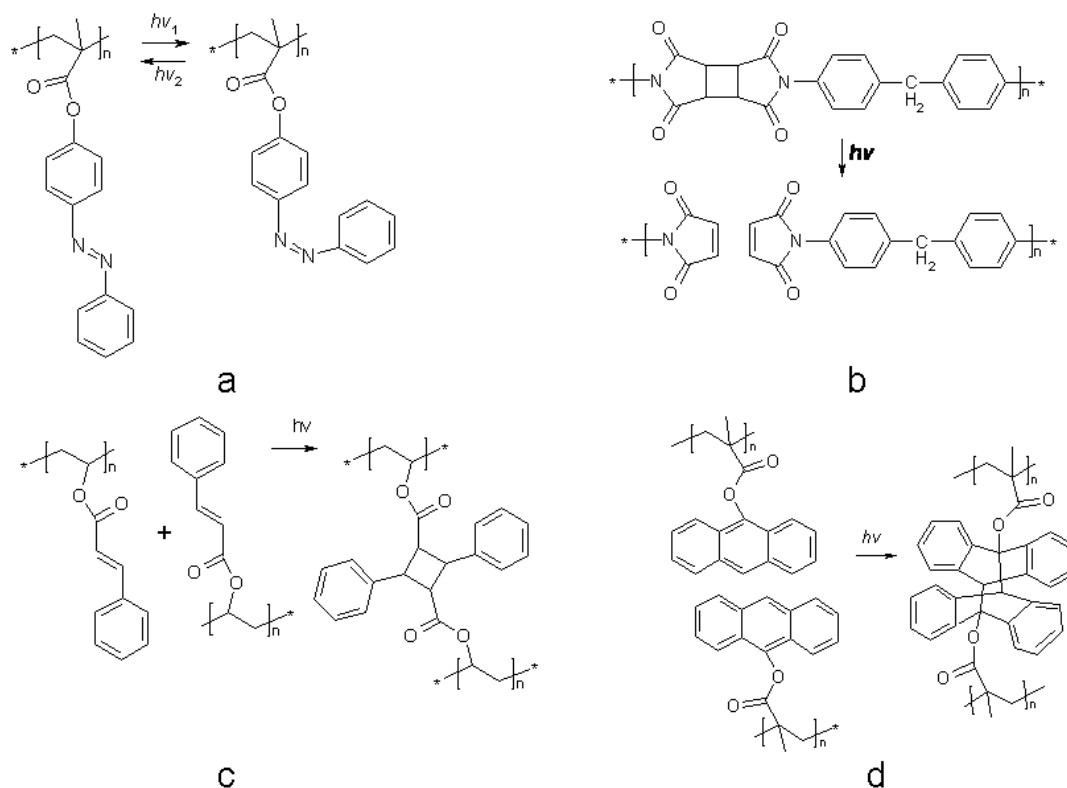


Figure 3. Examples of photochemical reactions leading to photoalignment: a – *trans-cis* isomerization of azobenzene fragments, b – photodecomposition of polyimide backbone, c – [2+2] cycloaddition of cinnamate fragments, d – [4+4] cycloaddition of anthracenyl fragments.

Comparing with the material discussed above, the photo-crosslinking materials demonstrate the best promise. They commonly combine rather good photosensitivity and high resistance of LC alignment to heat and light, because of irreversible photochemistry and strongly restricted molecular motions. Apparently, the aligning materials presented in the market [38, 39] belong to this class of materials.

1.5. Current trends

Recently, a thirty-year effort in development of photoalignment culminated in the first industrial application; based on photoalignment effect and proprietary materials, Sharp Corp. developed and commercialized method for production of LCD panels with multidomain vertical alignment (so called UV²A technology) [40]. The merits of UV²A panels are claimed to be the lower power consumption, higher contrast ratio, faster response and lower manufacturing cost.

The prospects of photoalignment technique for the displays with low-pret tilt alignment, *e.g.*, TN, STN, IPS LCDs, are not so clear. The earlier announced advances are still not industrialized [7,41]. Among the most urgent problems hindering application of photoalignment in this field is the material problem. The most important material issue is still alignment stability, such as photo- and thermal stability, and alignment aging understood as gradual alignment decay with a storage or operation time of LC cells. Besides, research efforts are also aimed at strengthening of sensitivity and improvement of dielectric characteristics of the photoaligning layers, to eliminate the residual DC (RDC) voltage and increasing the voltage holding ratio (VHR) of LC cells.

To solve these problems, different approaches are being currently tested. For commercial reason, not all of them are reflected in public literature. According to published data, several important trends can be selected. First of all, there is a tendency to search materials bearing photosensitive groups with a basically new photochemistry. For this purpose, new organic materials [42-45], plasma coatings [46], and even biomaterials [47] are being investigated. In addition, there is a clear trend in the use of materials capable of several types of chemical transformations. Typically, these transformations play different role in photoalignment. At least one of them is rather sensitive to light polarization so that it causes efficient photoordering. The other reaction(s) serves to stabilize this ordering. For example, paper [48] reports polyamic acid - azocopolymer configuration, in which orientational order achieved by the *trans-cis* transformations of the azo fragments is fixed by simultaneous imidization of the polyamic acid. Similarly, in papers [49,50] azomonomer is copolymerized with cinnamate monomer. The first of them provides pronounced photoordering via *trans-cis* isomerization, while the second one fixes this order via photo-crosslinking of the type of [2+2] cycloaddition. The same approach is applied to improve stability of LC photoalignment on sulfuric diazodyes [51], with the difference that the attached terminal groups of the dye were capable to photopolymerization. The combination of cinnamate and alkenyl reactive groups capable, correspondingly, of [2+2] cycloaddition and polymerization, is realized in [44]. Combining these groups, authors attained essential increase of light sensitivity and anchoring energy.

1.6. Our concept

The approach outlined in this article is based on several ideas. Firstly, we draw attention to a new type of photo-transformations – Fries rearrangements, which appear in a big number of organic materials bearing

aromatic groups. This type of photochemical reactions was first reported by Kobsa [52], and Anderson and Reese [53] upon UV irradiation of substituted phenyl acetates.

Figure 4 schematically presents a currently accepted mechanism of the photo-Fries rearrangement. On the first stage, UV irradiation leads to a homolytic cleavage of the acyloxy bond resulting in a pair of radicals trapped in a solvent cage. The radical pair then diffuses away from one another (“cage escape”) leading to the phenolic products or forms an enol, which undergoes tautomerization to yield hydroxyacetophenone products.

The photo-Fries rearrangement occurring in functional polymers bearing aryl ester moieties has also been intensively studied [54-57]. Guillet observed that photo-Fries active moieties in poly(phenyl acrylate) [55] and poly(naphthyl acrylate) [56] rearrange upon exposure to UV light in the range of 220-340 nm to give a polymer with pendant *ortho* and *para*-hydroxyacetophenone groups. The rearrangement was confirmed by the appearance of a new band in the absorption spectrum of the polymer at 340 nm corresponding to the $n \rightarrow \pi^*$ excitation of the hydroxyacetophenone group. Inherent change of polymer refractive index in photo-Fries rearrangement has recently led to the application of this rearrangement in developing polymers capable of adjustable refractive indices [57].

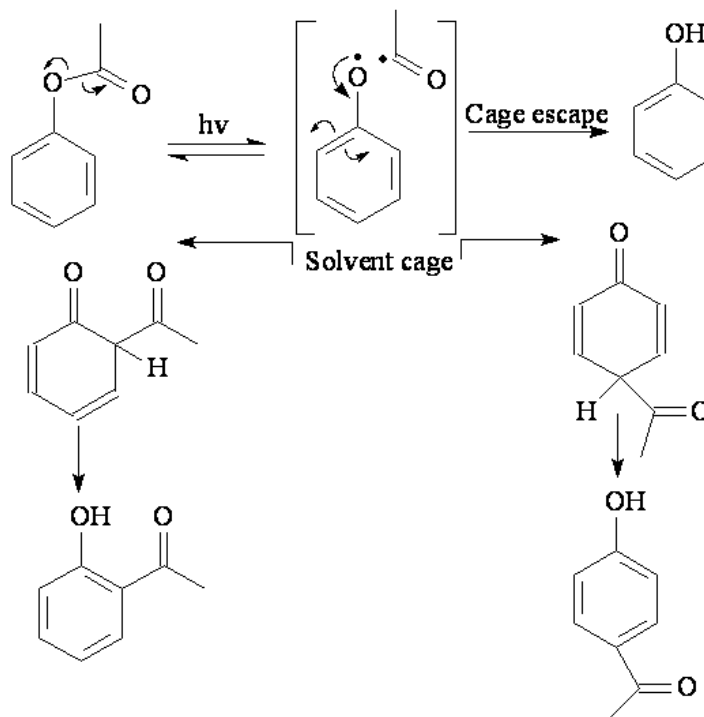


Figure 4. Mechanism of photo-Fries rearrangement.

The angularly selective photo-Fries conversion, occurring in polarized light, results in orientational ordering, which manifests itself in optical birefringence and dichroism [58]. We demonstrate that this ordering results in LC photoalignment. Since products of Fries reaction are irreversible and photostable [59], we have good chances to improve alignment stability. Besides, since presence of reactive double bonds increasing π -conjugation is not required, it is possible to shift molecular absorption to deep UV range. Thus, consideration of photo-Fries rearrangement as an order-generating reaction allows one to essentially expand the search field of photoaligning materials for industrial applications involving materials with totally new properties.

The second idea forming the basis of these studies is to combine photo-Fries rearrangement with other reactions stabilizing induced orientational order. This idea is realized by introducing tetrahydrophthalic/maleimide/methacrylamide groups capable of photo-crosslinking due to photocycloaddition or photopolymerization. It is important to note that these reactive groups are linked directly to photosensitive fragment that can fix better their orientational ordering. The classes of polymers falling under this concept are discussed in our earlier works [60-64]. The present paper reviews and systematizes these data and brings number of new results confirming effectiveness of our strategy.

2. Experimental details

2.1. Material synthesis and characterization

The brief description of the synthesis of each type of materials is presented in sections 3-6. The details of these syntheses can be found in our earlier works [60-66]. Thin layer chromatography and ^1H NMR spectroscopy were employed to determine the purity and the chemical structure of the obtained materials. Thin layer chromatography was performed on Merck Kieselgel plates 60-F254. ^1H NMR spectra were recorded by a Varian 400 NMR spectrometer with the use of tetramethylsilane in a DMSO-d_6 solvent as an internal standard. In some cases IR spectroscopy studies were additionally involved to identify and characterize structures of synthesized compounds (see part 2.3).

The polymerization kinetics was monitored in dilatometry studies. The kinetic curves were obtained at the following conditions assumed as standard ones for all monomers discussed: 5 wt. % solution of monomer in DMF, presence of 1 wt. % of AIBN initiator in the monomer, inert atmosphere (argon), temperatures 60° , 70° and 80° C.

2.2. UV spectroscopy studies

These studies were conducted to elucidate mechanisms of photochemical transformations in monomers and polymers based on them. Besides, polarized UV/Vis spectra were measured to characterize photoinduced ordering in these materials.

Spectra of monomers were measured for the solutions of these monomers in ethanol (concentration of monomers 10^{-4} - 10^{-5} mol/l) with Specord UV/Vis spectrophotometer. As a source of irradiation of examined compounds we used a high-pressure Hg lamp DRS-500 (Russia). The integral light intensity was about 80 mW/cm^2 , and the exposure time was 15-30 min. The formation of oxyketone structures was identified with a new long-wave absorption maximum.

The UV/Vis spectra of polymers were measured for both solutions and films using an S2000 diode array spectrometer from Ocean Optics. The polymers were dissolved in DMF, THF, dichloroethane or toluene. The spectra in solution were measured for the solutions with polymer concentration 10^{-4} - 10^{-5} mol/l placed in a quartz cuvette ($l=1 \text{ cm}$). The polymer films were prepared by spin coating 5-10 wt. % solution of chosen polymer onto slides of fused quartz. Subsequently, the films were baked at 100°C for 1 h to complete evaporation of solvent remained after coating procedure. For UV illumination we used the full emission spectrum of a high-pressure mercury lamp DRS-500. To study the photochemical changes in polymers, the samples were illuminated by a non-polarized light with an integral intensity of 105 mW/cm^2 . For the anisotropy induction, the polymer films were illuminated with the light linearly polarized by Glan-Thompson prism. The polarized light intensity was about 40 mW/cm^2 . The exposure time was varied from 5 to 120 min.

2.3. IR spectra measurements

The FTIR spectra of polymer films were measured to characterize synthesized structures and clarify mechanisms of photochemical transformations. The spectra were measured in the spectral range $380\text{--}4000 \text{ cm}^{-1}$ with a resolution of 2 cm^{-1} by using Bruker IFS-66 FTIR spectrometer. The polymer films were obtained by spin coating the polymer solutions on the KBr plates and subsequent backing at 100°C over 1 h for the completion of solvent evaporation. The films were exposed to unpolarized UV light as described in the previous subsection.

2.4. LC cells and photoalignment tests

The LC cells have been made in a standard way. The 1 wt. % solution of photoaligning polymer in DMF was spin coated on ITO covered glass plates. The films were subsequently backed at 150°C over 1 h. The photoalignment processing was realized by using high-pressure mercury lamp DRS-500, whose irradiation was linearly polarized by a Glan-Thompson prism. To impart unambiguous direction of LC pretilt, the substrates were irradiated in two steps: first with polarized UV light (15-40 mW/cm², 5-30 min) and then with non-polarized UV light (7-100 mW/cm², 0.5-1.0 min) by rotating the sample at 90° around its normal. In the first phase, sample was irradiated at normal light incidence, while in the second one the light was directed obliquely at the incidence angle of 45°. Typically, the substrates were irradiated through a mask opening only the central rectangular area of the substrates. This made it possible to compare the alignment in exposed and unexposed areas.

Two types of LC cells were constructed. In the most common case, LC cell was made by sandwiching LC between a pair of glass/ITO slides (substrates) coated with photoalignment layer and irradiated as described above. To obtain a uniform director orientation across the cells, the substrates were assembled in an antiparallel fashion meaning that directions of irradiation with non-polarized light were antiparallel to each other. Cell thickness was adjusted by spacers with a diameter of 20 μm. These cells, called symmetrical cells, were used to determine the type of LC alignment (homeotropic, planar or tilted), and also to measure pretilt angle of LC. In addition to antiparallel symmetric cells, twisted symmetric cells were made, in which easy alignment directions on the opposite substrates were perpendicular and a cell thickness was 6 μm. These cells were used for electro-optic tests.

To define alignment direction in the cell plane and the value of azimuthal anchoring energy, we also constructed cells consisting of rubbed polyimide substrate and a photoaligned substrate (asymmetrical cells). The easy axis of the photoalignment substrate was turned in 90° with respect to the rubbing direction of the polyimide substrate. The rubbed substrate was used as a reference one with predetermined alignment direction and strong azimuthal anchoring. The thickness of these cells was reduced to 6 μm to increase higher measurable value of azimuthal anchoring energy.

The cells were filled at room temperature or in isotropic phase with various nematic LCs from Merck with positive (5CB, E7, ZLI2293, ZLI4801-000) and negative (MJ961180 and MLC6609) dielectric anisotropy. We judged the alignment quality by cell observation in a light box and

polarizing microscope using evaluation scale with five grades: (1) excellent; (2) good (single alignment faults); (3) satisfactory (minor alignment faults); (4) bad (big number of alignment faults in a form of inversion walls, flowing patterns, etc.) and (5) no alignment. Also, similarly to [44], alignment quality of antiparallel cells was additionally evaluated by measuring transmittance oscillations of these cells placed between crossed polarizers during their rotation around the axis normal to the cell plane. The parameter

$$q = \frac{T_{\max} - T_{\min}}{T_{\max}}, \quad (2)$$

where T_{\max} and T_{\min} are maximal and minimal values of oscillating transmittance, was used as a measure of alignment quality. It will be called below the quality parameter. It describes the LC alignment quantitatively, but does not give its full assessment. Because of this, for a more complete description, we usually combine q and alignment grade according to the scale above.

The pretilt angle was measured by a conventional crystal rotation method, while azimuthal anchoring coefficient was estimated by spectroscopic method described in [67].

3. Poly(1-naphthyl methacrylate)

In the next four sections, we successively describe the classes of materials developed under the above concept. The order of discussion of these classes corresponds to the historical sequence of their investigation. At the same time, this order reflects milestones and logic of our research aimed at improvement of photoaligning properties.

We begin by considering the aligning properties of poly(1-naphthyl methacrylate) (**pNMA**). The discovered good photoaligning ability of this material hinted at an important role of photo-Fries rearrangements in the photoordering process and inspired us to extensively explore the area of materials capable of Fries photoreaction.

3.1. Polymer syntheses and photochemistry

The **pNMA** ($T_g = 135^\circ\text{C}$) was obtained by simple radical polymerization of 1-naphthyl methacrylate in DMF solution with AIBN as initiator [60].

The UV/Vis spectra of **pNMA** in toluene solution and films were measured before and after irradiation. The **pNMA** spectra in the solution are presented in Fig. 5. There is evident that UV exposure leads to a decrease in

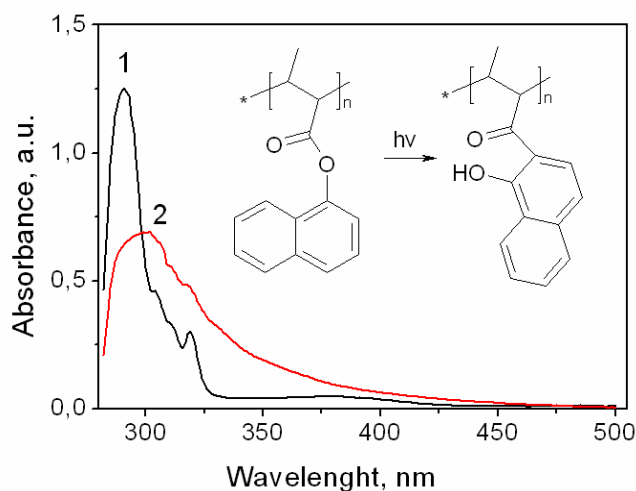


Figure 5. UV/Vis spectra of **pNMA** in toluene solution: 1 – before irradiation; 2 – after irradiation (25 mW/cm², 15 min). Inset: scheme of photo-Fries rearrangement.

the most intensive band centred at about 290 nm and associated with $\pi \rightarrow \pi^*$ and $n \rightarrow \pi^*$ transitions of naphthyl fragments, and, simultaneously, an increase in absorption in the long-wave region of the spectrum. These changes are typical for photo-Fries photorearrangement in organic materials [55,56].

3.2. LC alignment

In the cells of various type based on **pNMA** aligning layers we observed LC alignment of rather high alignment quality (excellent/good grade, $q=0.85-0.95$). As an example, Fig. 6 shows the alignment of LC ZLI 4801-000 in antiparallel symmetric cell.

Depending on LC and exposure dose, the induced pretilt angle was 0.5°-1.0°. The azimuthal anchoring energy showed growth with exposure dose with a clear tendency of saturation. The saturation value was $(5-10) \times 10^{-6}$ J/m², *i.e.*, rather high for photoaligning materials.

Unfortunately, along with high quality, LC alignment on **pNMA** demonstrated rather poor thermal stability. Even upon aging the cells at temperature 90°C, which is lower than the temperature of nematic-isotropic transition, and significantly lower than the glass transition temperature of **pNMA**, we observed gradual decay of LC alignment. The full decay was observed for about 20 min of aging. The degradation of LC alignment can not be caused by reversible photochemistry, since Fries isomers are very stable [59]. The possible reason of this can be orientational disordering of the initially photoordered naphthyl fragments and their Fries isomers at elevated temperatures. Indeed, at temperatures close to T_g the frozen photoinduced

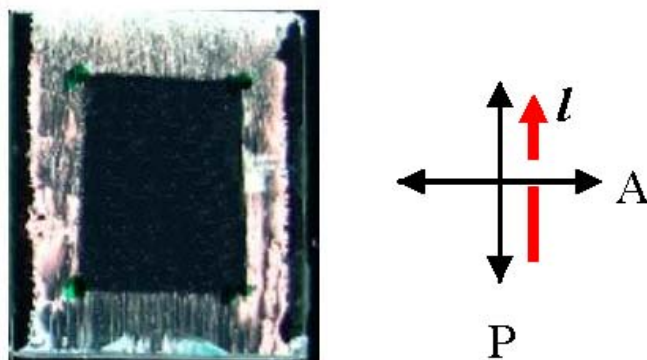


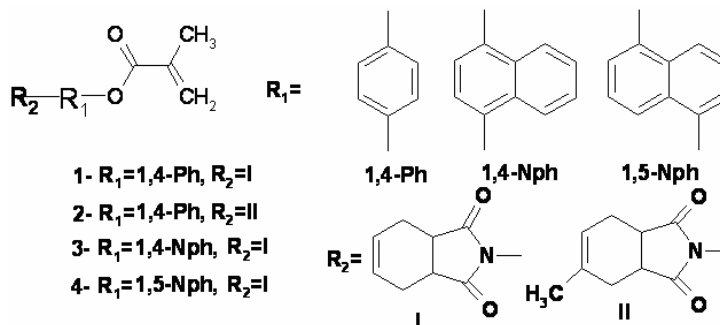
Figure 6. Photograph of symmetric antiparallel cell based on **pNMA** aligning layers and filled with nematic LC ZLI4801-000. The scheme on the right shows position of polarizer, P, analyzer, A, and alignment direction, *I*.

order melts, since increasing free volume of polymer provides new degrees of freedom for the polymer chains.

To eliminate this disordering process and thus to stabilize LC alignment, we have developed multifunctional monomers with several active groups in the molecule; along with the groups capable of Fries rearrangements we introduced the groups with reactive C=C bonds capable of dimerization or polymerization. The key role of the latter groups was to fix orientational order induced mainly due to Fries photo-conversion. The substituted arylmethacrylates with reactive double bond in tetrahydrophthalic (section 4), maleimide (section 5) and methacrylamide group (section 6) were developed and used as starting monomers for the syntheses of advanced photoactive polymers.

4. Tetrahydrophthalimidophenyl- and naphthyl methacrylates

These monomers are aryl methacrylates with an additional reactive C=C bond located in tetrahydrophthalimide fragments I- II:



The polymers corresponding to monomers **1**, **2**, **3** and **4** will be denoted **poly-1**, **poly-2**, **poly-3**, and **poly-4**, respectively. In the monomers above, more active C=C bond in methacryloyl group can be polymerized by common radical process. The obtained soluble linear polymers can be further crosslinked due to photoreaction of C=C bonds in tetrahydrophthalimide fragments. Besides, under irradiation, photo-Fries reaction occurs in these polymers.

4.1. Syntheses

Synthesis of the monomers was carried out in two stages. Starting hydroxyphenyl/naphthyl imides/amides were synthesized by condensation reaction of 4-aminophenole or 4-aminonaphthole and 1,2,3,6-tetrahydrophthalic anhydride/ 5-methyl-3,4,7,7-tetrahydro-phthalic anhydride at presence of sodium acetate in acetic acid as a solvent. Condensation was carried out at the temperature of boiling point of acetic acid. 5-Hydroxynaphthylamide was obtained in 1,4-dioxane solution at boiling point of 1,4-dioxane. On the second stage, monomers **1-4** were obtained by heating the appropriate initial imides/amides with excess of methacrylic anhydride and catalytic amount of H₂SO₄ and phenotiazine as an inhibitor of polymerization. The structures of the synthesized substances were characterized using ¹H NMR, IR and UV-spectroscopy.

Monomers **1-4** were polymerized by thermoinitiated radical polymerization. The polymerization was carried out in N,N-dimethylformamide (DMF) solutions (at 10 wt. % concentration of monomer) at 80°C with AIBN as initiator. It was found that during the polymerization the non-substituted tetrahydrophthalimide units (R₂=H) in monomers **1**, **3**, and **4** readily crosslink so that linear soluble polymer products could only be obtained at low monomer conversions (~20 wt. %). In a case of monomer **2**, one can reach higher yield of soluble polymer (up to ~40 wt. %) due to less activity of methyl-tetrahydrophthalimide unit. Molecular weights estimated for soluble poly-(tetrahydrophthalimidophenyl- and naphthyl methacrylates) by GPC (eluent chloroform:ethanol = 95:5, polystyrene standards) were in the ranges: $M_n = 140\ 000 - 199\ 000$, $M_w = 216\ 000 - 266\ 000$. As an illustrative example, detailed description and characterization of monomer **1** and its polymer **poly-1** is given at the end of this section.

We have further recognized a direct influence of temperature on the yield of non-crosslinked polymer products: at lower temperature (60° C) soluble polymer products were obtained with higher yields: ~25 wt. % for **poly-1**, and ~35 wt. % for **poly-3** and **poly-4**). To get more details of this dependence,

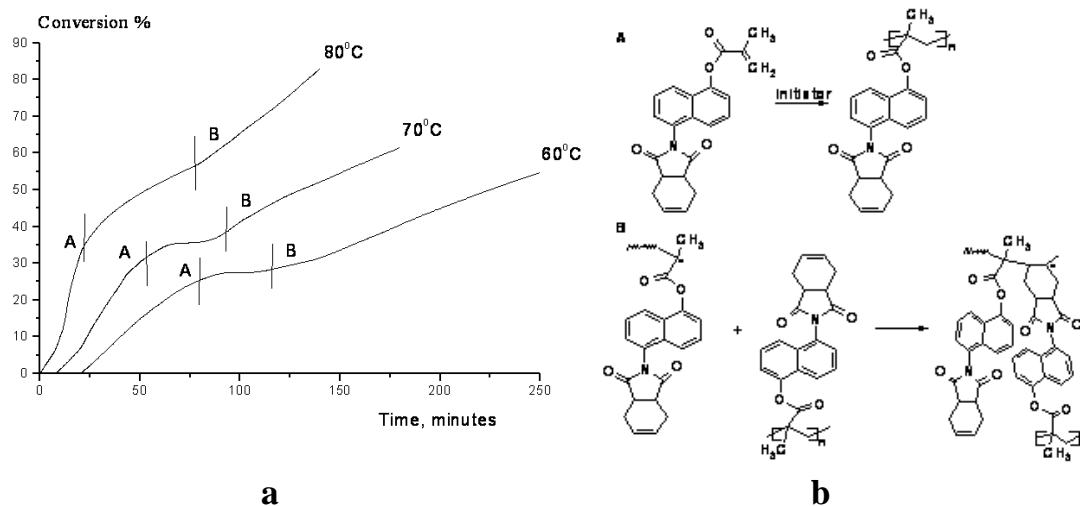


Figure 7. The kinetic curves of thermally initiated radical polymerization of monomer **4** at 60°, 70° and 80° C (a) and schematic representation of polymerization/crosslinking processes corresponding to A and B parts on the curves.

thermally initiated polymerization of the monomers was investigated with dilatometry. For illustration, Fig. 7 presents kinetic curves obtained for monomer **4**. Two quasilinear parts of these curves, A and B, can be selected. The part A corresponds to linear polymer product formation, while the part B reflects formation of crosslinked products due to involvement of second C=C double bond of tetrahydrophthalimide fragment in the polymerization process. This shows that it is very important to interrupt in time the polymerization reaction to prevent formation of a large number of crosslinked products.

In conclusion, it should be noted that recently we increased the polymerization yield of monomers **1** and **2** to ~40 wt. % by photopolymerization at room temperature [64]. However, this method is not universal. For example, it is ineffective for monomers **3** and **4**, because of radical trapping by naphthalene fragments. Nevertheless it shows promising way towards effective synthesis procedure for this class of photoaligning polymers.

Synthesis example

Synthesis of monomer 1. Starting 4-hydroxyphenylimide was synthesized by condensation reaction of the equimole amounts of 4-aminophenole and 1,2,3,6-tetrahydrophthalic anhydride at the presence of the equimole amount of sodium acetate in acetic acid as a solvent. The condensation was carried out at the temperature of boiling point for acetic

acid in glass reactor with a condenser during 5 hours. After crystallization in isopropyl alcohol, colourless crystals of 4-hydroxyphenylimide were obtained (m.p.=242°-244° C, yield of the monomer 25.9 wt. % (with respect to started 4-aminophenole)). 4-Hydroxyphenylimide was heated to 80°-90° C with 30 wt. % excess of methacrylic anhydride and catalytic amounts of H₂SO₄ and phenotiazine. After completion of this reaction, the resulting mixture was poured into water. Crystallization was carried out in a toluene-hexane (1:1) mixture with silica gel. Colourless amorphous monomer **1** was obtained (m.p. = 137-138°C). ¹H NMR identification (100 MHz, acetone-d₆), ppm: 7.32 (s, 4H, Ar), 6.32 (s, 1H, =CH₂), 5.98 (m, 2H, =CH), 5.85 (s, 1H, =CH₂), 3.34 (s, 2H, CH), 2.54 (d, 4H, CH₂), 2.06 (s, 3H, CH₃). IR identification (KBr), cm⁻¹: broad 3080 (C-H), 3040 (C-H), 1730 (C=O), 1690 (N-C=O), 1630 (C=CH₂), 1635 (HC=CH), 1600 (Aryl), 1510(Aryl), 1455 (Aryl), 1290, 1140 (C-O), 890 (=CH), other signals 820, 710. UV spectrum (ethanol, c= 2x 10⁻⁵ mol/l): λ_{max 1} = 220 nm, ε_{max 1} = 2.05x 10⁴ (l/(molxcm)) and λ_{max 2} = 282 nm, ε_{max 2} = 0.525x 10⁴ (l/(molxcm)).

Synthesis of polymer poly-1. 0.14 g of monomer **1** and 0.0014 g of azobisisobutyronitrile (AIBN) were dissolved in 1.5 ml of DMF. The reaction vessel with the solution was subsequently closed air-tight. The solution was heated to 60°C for 60 min. Thereafter, the reaction vessel was opened and the solution was added dropwise to 20 ml of ethanol while stirring at room temperature. The separated polymer was filtered off, dried, dissolved in 1 ml of DMF and this solution was added dropwise to 10 ml of ethanol. Filtration and drying at 40°C in a vacuum gave 0.032 g (23 wt.%) of **poly-1**. GPC (eluent chloroform:ethanol = 95:5, polystyrene standards): M_n= 199 000, M_w = 256 000. M_w/M_n=1.3.

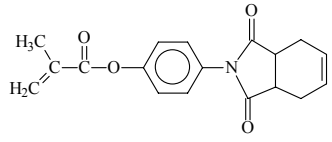
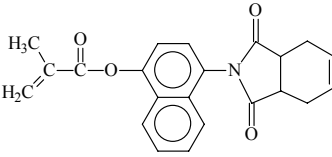
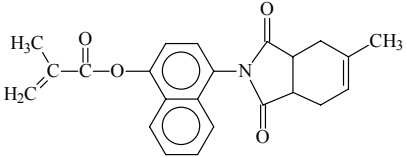
4.2. Photochemistry: UV/Vis spectroscopy studies

Photo-Fries rearrangement in the monomers was confirmed by the appearance after UV-irradiation of a new band at around 370 nm in the absorption spectra of their ethanol solutions, both for phenylene- and naphthalene containing monomers (R₁= 1,4-Ph, 1,4-Nph, 1,5-Nph).

4.3. LC alignment

The photoinduced LC alignment with a quality grade “excellent” or “good” in both parallel and 90° twist configuration was recognized only for materials with 1,4-substituted aromatic core (R₁= 1,4-Ph, 1,4-Nph) presented in Table 1. As well as for **pNMA**, easy axis of LC alignment was induced

Table 1. Characteristics of LC alignment for the best polymers with tetrahydrophthalimide fragments.

Monomer structure	Alignment quality	Alignment quality parameter
	good/excellent	0.88-0.95
	good	0.85-0.90
	good	0.85-0.92

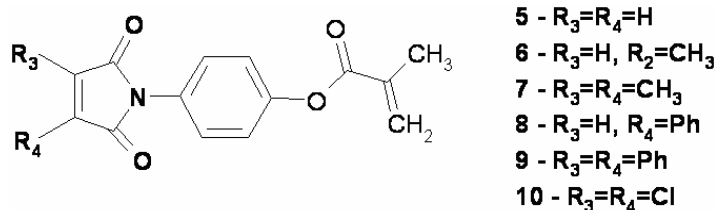
perpendicularly to the direction of light polarization E . The pretilt angle and anchoring energy values were similar to **pNMA**.

The induced alignment was quite stable at 90°C; for LCs with the nematic-isotropic phase transition above 90°C, it was kept for 3-5 hours of our monitoring. However, the alignment degraded rather fast at 110°C, when LC was in isotropic phase. In this case, the decay time of LC alignment was only about 10 min.

Thus, comparing with **pNMA**, this class of materials demonstrates improved thermal stability. However, the stability was still rather poor for practical use of these polymers. The lack of stability can be explained by low crosslinking rate, caused by insufficient reactivity of C=C bonds in tetrahydrophthalimide fragments.

5. Maleimidoaryl methacrylates

To increase crosslinking efficiency, tetrahydrophthalimide group was replaced by another active group, maleimide group, which also contains reactive C=C bond. The maleimide and methacryloyl groups were linked through aryl spacer. The naphthyl spacer giving worse result (see 4.3) was not used in these syntheses. The general formula of the synthesized monomers is as follows:



As in the previous case, these materials contain two $C=C$ bonds with different reactivity. The more active $C=C$ bond in methacryloyl group can be polymerized *in vitro*, in a process of polymer synthesis. In turn, the weaker $C=C$ bond in maleimide group can be photopolymerized *in situ*, *i.e.*, during photoalignment processing of the polymer film.

5.1. Syntheses

Synthesis of the monomers was carried out in two stages [66], just as for monomers of previous class. The structures of the synthesized substances were characterized using 1H NMR spectroscopy.

In order to obtain polymers **poly5-poly10**, the corresponding monomers **5-10** were polymerized at $80^\circ C$ in DMF solutions at 10 wt. % concentration of monomer with AIBN as initiator. The monomers **5** and **6** were found to form polymers with crosslinked structure at low rate of monomer conversion preventing the formation of linear (soluble) polymer. For the monomer **5** soluble polymer fraction was obtained with very low yield and in only some syntheses. For the compound **6** linear polymer was reproducibly obtained at the monomer conversions less than 10 wt. %. In case of monomers **7** and **8** soluble polymer products were obtained at higher monomer conversions, 15-20 wt. %. Monomer **9** with 2,3-diphenylmaleimide fragment could be converted into soluble polymer with even higher conversion ~ 40 wt.%. Conversely, for monomer **10**, which releases Cl during polymerization and traps free radicals, soluble polymer **poly-10** was obtained at monomer conversion less than 10 wt. %.

Based on results of GPC (eluent chloroform:ethanol = 95:5 or DMF, polystyrene standards) measurements for soluble **poly-6-poly-10** molecular weights were estimated; $M_n = 102\ 000 - 461\ 000$, $M_w = 130\ 000 - 928\ 000$.

The example below illustrates synthesis procedure for this class of polymers.

Synthesis example

Synthesis of monomer 6: Starting 4-hydroxyphenylimide was synthesized by condensation reaction of the equimole amounts of 4-aminophenole and

citraconic anhydride in acetic acid at boiling point of acetic acid in glass reactor with a condenser during 1 hour. After crystallization in isopropyl alcohol colourless crystals of 4-hydroxyphenylmaleimide were obtained (m.p.= 175°C, yield ~80 wt.%). 4-Hydroxyphenylmaleimide was heated at 90° C with double excess of methacrylic anhydride with catalytic amounts of H₂SO₄ and phenotiazine. After 4 hours, the resulting mixture was poured into water. Crystallization was carried out in a toluene-hexane (1:1) mixture with silica gel. Colourless amorphous monomer **6** was obtained (m.p. = 128°C, yield ~ 60 wt.%). ¹H NMR identification (100 MHz, acetone-d₆), ppm: 7.52-7.25 (m, 4H, Ar), 6.68 (s, 1H, =CH), 6.33 (s, 1H, =CH₂), 5.88 (s, 1H, =CH₂), 2.12 (s, 3H, CH₃), 2.05 (s, 3H, CH₃).

Synthesis of polymer poly-6: 1g of monomer **6** and 0.001g of AIBN were dissolved in 10 ml of DMF. The solution was heated at 60°C for 60 minutes in the subsequently closed air-tight vessel. Thereafter, the reaction solution was added dropwise to 20 ml of acetone while stirring at room temperature. Filtration and drying at 40°C in a vacuum gave 0.1535 g (~15 wt. %) of **poly-6**. GPC (eluent DMF, polystyrene standards): M_n= 461 000, M_w = 928 000. M_w/M_n=2.0.

5.2. Photochemistry: UV/Vis and IR spectroscopy studies

Spectra of monomers were studied by UV spectroscopy. In this case, we measured the spectra of monomers, dissolved in ethanol before and after irradiation with UV light. After the irradiation, broad absorption band around 320-330 nm was observed, which indicated the photo-Fries rearrangement.

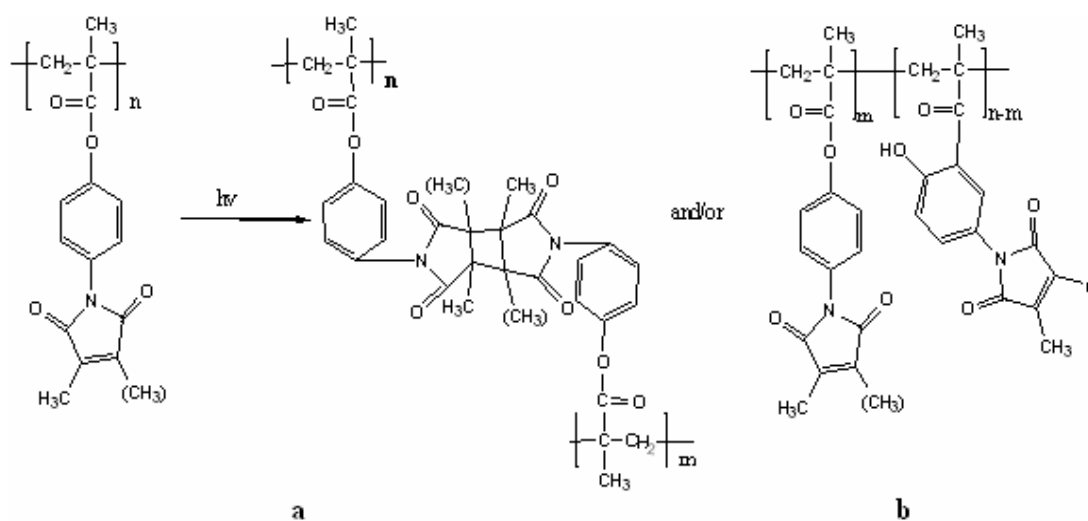


Figure 8. Schemes of (a) [2+2] photocycloaddition and (b) Fries rearrangement of the molecules of maleimidoaryl methacrylates.

The long-wave absorption increase after UV irradiation was also observed in the polymer films. This indicated Fries reaction in a solid state of the polymers. The changes in polymer films under UV light were also studied by IR spectroscopy. The photo-crosslinking reaction was detected by changes in vibration bands of maleimide moieties. In particular, the band at 850 cm^{-1} demonstrated pronounced decrease giving evidence of [2+2] photocycloaddition occurring between two maleimide moieties. The appearance of new absorption band at 1680 cm^{-1} indicated formation of ketone structures as products of Fries reaction. Thus, both [2+2] photocycloaddition and Fries rearrangement reactions, theoretically possible in these polymers, actually realize under UV irradiation. Schemes of these reactions are shown in Fig. 8.

5.3. LC alignment

The alignment quality results for these polymers are summarized in Table 2. It can be seen that the range of the alignment quality parameter is rather broad. One can observe some correlation between the alignment quality and the end substituents R_3 and R_4 in maleimide groups. For short substituents ($R_{3,4}=H, CH_3$) the alignment quality is better than for the longer one. Furthermore, for asymmetric maleimide structures ($R_3\neq R_4$) the alignment is better than for symmetric one ($R_3=R_4$). The former observation can be explained by steric hindrance caused by long and bulky substituents, which lowers yield of [2+2] photocycloaddition. This is indirectly confirmed by the fact that the crosslinking reaction is much more intensive in polymerization of monomers **5** and **6**, having small H and CH_3 substituents, than in monomer **9** with bulky aryl substituents (see section 5.1).

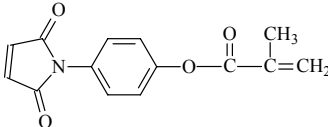
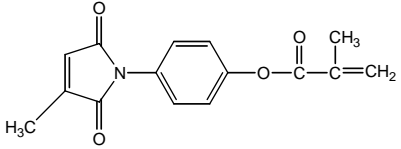
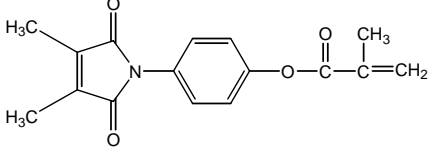
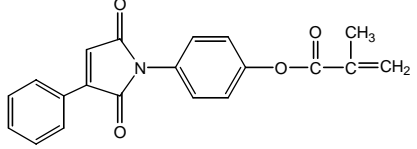
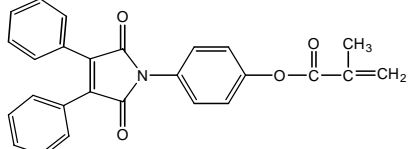
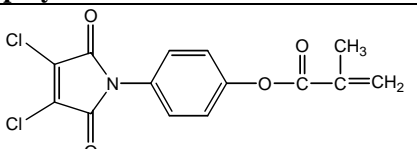
The bulky terminal groups may also reduce yield of Fries reactions, because under conditions of limited free volume of polymers, they hamper molecular rearrangements associated with significant steric changes. The higher alignment grade in case of asymmetric maleimide structures might be explained assuming that R_3 and R_4 fragments influence $C=C$ bond energy. Possibly, at $R_3\neq R_4$, this bond is weaker so that the yield of [2+2] photocycloaddition increases. This hypothesis will be tested in the future studies.

It should be noted especially high alignment quality obtained for **poly-6**. The end substituents R_3 and R_4 in this polymer seem to be well optimized from the view point of photoreactivity and LC photoalignment. The excellent alignment capability of this polymer is additionally illustrated by Fig. 9. The pretilt angle on this aligning polymer falls in the range $0.2\text{-}1.0^\circ$, and azimuthal anchoring coefficient exceeds 10^{-5} J/m^2 . The alignment endured 5 h

backing at 100°C. This altogether makes this polymer and similar structures rather promising for industrial applications.

At the same time, these materials have some weak points. One of them is insufficient reproducibility of synthesis; the materials are usually obtained with different polymerization yield that influences LC alignment. The most promising structure **poly-6** cannot be sufficiently modified that makes difficult further improvement of this polymer.

Table 2. Characteristics of LC alignment for some polymers with maleimide fragments.

Monomer structure and polymer marking	Alignment quality	Alignment quality parameter
 <p>poly-5</p>	excellent/ good	0.9-0.96
 <p>poly-6</p>	excellent	0.95-0.98
 <p>poly-7</p>	good/ excellent	0.88-0.96
 <p>poly-8</p>	good	0.86-0.94
 <p>poly-9</p>	bad/satisfact.	0.6-0.8
 <p>poly-10</p>	bad	0.4-0.6

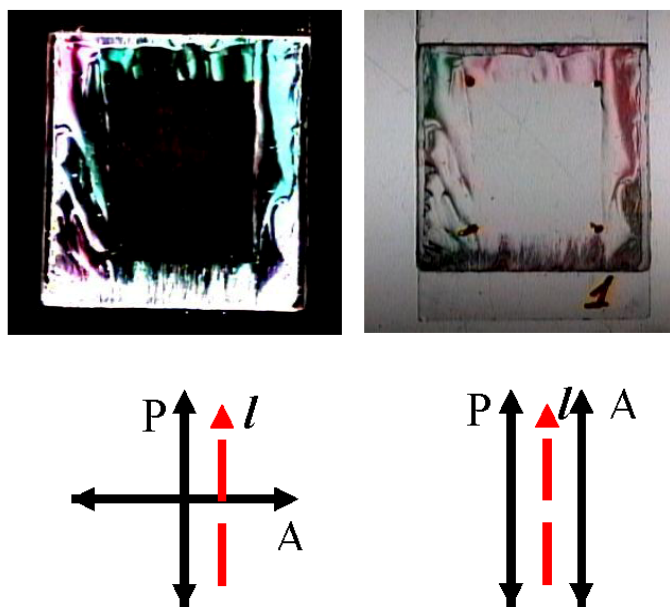


Figure 9. Photographs of symmetric antiparallel cell based on **poly-6** aligning layers and filled with nematic LC E7. The schemes below show position of polarizer, P, analyzer, A, and alignment direction, *l*.

6. Methacrylamidoaryl methacrylates

Development of these materials is a culmination point of the present research. In the materials above the photoalignment treatment resulted in conversion of $C=C$ bonds located in the bulky cyclic groups. We believed that the bulky photoproducts are less mobile than the small one, leading to an increase in thermal stability of the induced alignment. As shown above, this idea has been partially correct. However, the above discussed synthesis problems and constrains in polymer modification stimulated us to change direction of research. The cycling crosslinkable groups we decided to replace by small methacryloyl groups capable of radical polymerization. In other words, we switched to the class of polyarylmethacrylates containing non-polymerized methacryloyl groups. The general formula of these polymers and their possible photoproducts are shown in Fig. 10.

Normally, these polymers were obtained by radical polymerization of corresponding monomers, same as the polymers of other classes discussed above. The monomers were methacryloylamidoaryl-methacrylates having two methacryloyl groups of different reactivity (Fig. 11). The more active *O*-methacryloyl group was subjected to polymerization in a synthesis process, while the less active *NH*-methacryloyl group underwent crosslinking reaction due to polymerization process under UV irradiation or heating.

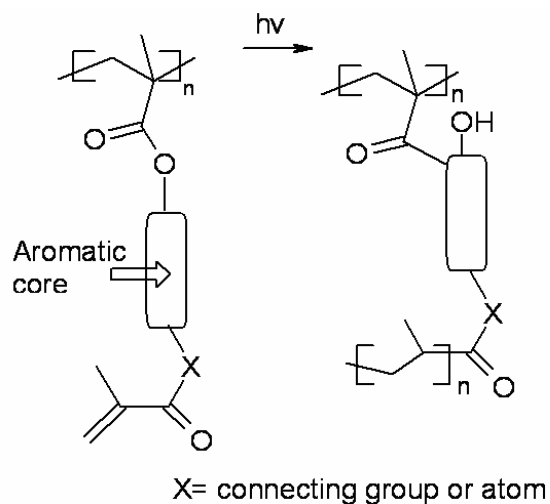


Figure 10. General formula of methacrylic polymers with free methacryloyl group.

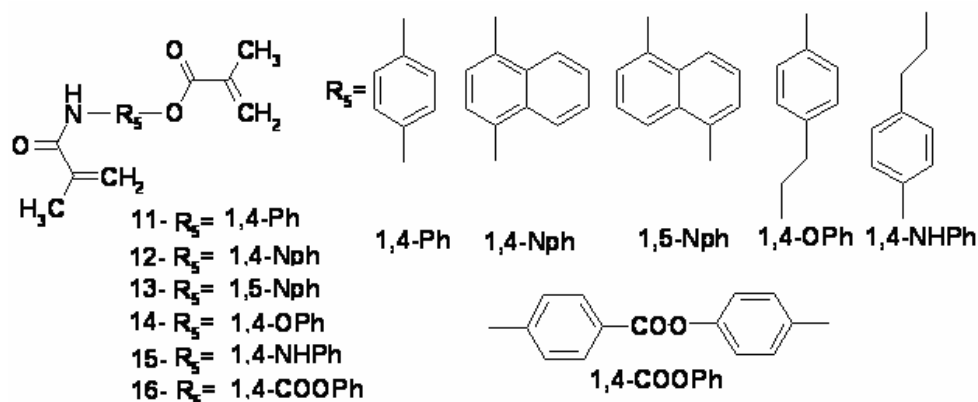


Figure 11. Structures of synthesized methacrylamidoaryl methacrylates.

In addition to direct polymerization, some of these structures were obtained by polymer-analogue reaction. The advantages and weak points of these two synthesis approaches are discussed in the next subsection.

6.1. Syntheses

Synthesis of the monomers was carried out in one or two stages by acylation of 1,4-aminophenole (monomer **11**), 1,4- and 1,5-aminonaphthole (monomers **12** and **13**), tyramine (monomer **14**) or 4-amino-phenethyl alcohol (monomer **15**) with methacrylic anhydride or methacryloyl chloride. Monomer **16** was prepared in three stages: p-hydroxy benzoic acid and 1,4-

aminophenole were acylated with methacryloyl chloride and obtained intermediates were condensed using DCC/DMAP activating reagents. The structures of the synthesized substances were characterized using ^1H NMR, IR and UV-spectroscopy.

Monomers **11-16** were polymerized by radical polymerization in DMF solutions (10 wt. % concentration of monomers) with AIBN as initiator at 80°C . It was found that naphthalene-containing monomers **12**, **13** could be radically polymerized into soluble polymer products **poly-12**, **poly-13** up to 70 wt. % monomer conversion. Instead, maximum yield of soluble polymers **poly-11**, **poly-14** and **poly-16** for phenylene-containing monomers **11**, **14**, **16** falls down to 30 wt. % of monomer conversion. Soluble polymer **poly-15** could be obtained at 15 wt. % conversion of monomer **15**.

For all polymers obtained the molecular weight distribution is bimodal consisting of a higher molecular weight fraction (for which M_w , M_n and M_w/M_n values are derived) and a broad lower molecular weight fraction. The GPC results presented in Table 3 for **poly-11**, show quasilinear grows of polymer weight with the yield of polymerization. The values of M_n and M_w obtained for **poly-11–poly-16** were in the ranges: $M_n= 16\ 500\text{--}33\ 600$, $M_w=49\ 400\text{--}60\ 000$.

Monomers **11** and **16** were also copolymerized with monomers bearing hydrophobic tails using the same method; one of these monomers was dissolved in DMF together with methylmethacrylate, butylmethacrylate, 2,2,3,3-tetrafluoropropylmethacrylate (**MF-1**) or 2,2,3,3,4,4,5,5-octafluoropentylmethacrylate (**MF-2**) in appropriate molar ratios (1:1, 1:2, 2:1, etc.), doped by AIBN and kept at 80°C up to 10-30 wt. % of monomer conversion.

Table 3. GPC data, polymerization yield, and alignment quality grade for **poly-11**.

Polymer yield, wt. %	M_w	M_n	M_w/M_n	Low molecular weight fraction, wt. %	Alignment grade
12	29 400	12 600	2.3	12	excellent
23	50 500	28 600	1.8	36	good
35	60 000	33 600	1.9	22	excellent/ good

* GPC-measurements were performed using PSS-SDV columns and DMF eluent containing LiBr at a flow rate of 1.0 mL/min. The calibration curves for GPC analysis were obtained using PSS polystyrene standards (1000 – 400000 D).

Given that selective polymerization of *O*-methacryloyl groups in monomers **11-16** is limited by low yield of soluble polymer product, we have also tried to explore another synthesis way; polymer materials with analogues structural elements were synthesised by polymer analogue reactions starting from poly(methacrylic acid). However, we realized that transformation of free carboxylic *-COOH* groups in poly(methacrylic acid) ($M_n=43\ 400$, $M_w = 75\ 600$) is limited in this reaction to 40 mol %. This means that no more than 40 mol % of photoactive fragments can be introduced. Representative of such polymers is a polymer **P1** the synthesis of which is described below.

Each of these synthesis methods has strengths and weaknesses. The monomer polymerization method provides maximal concentration of photosensitive fragments. However, because of similar reactivity of methacrylate and methacrylamide groups, it is hard to prepare soluble polymer with high monomer conversion yield; in fact, it is less than 30-40 wt. %. Moreover, the obtained structures are not pure; according to ^1H NMR spectra, even at monomer conversion 15-20 wt. %, these polymers have free *C=C* bonds of both methacrylamide and methacrylate types. Also, these polymer products contain fractions with high and low molecular weight. One way to improve synthesis of these polymers, which we now develop, is the use of monomers with increased difference in reactivity of terminal groups containing *C=C* bond.

The polymers prepared by polymer analogues reactions obviously have only one type of *C=C* bonds. The disadvantage of this approach is insufficient replacement of *-COOH* groups with photosensitive fragments (monomer conversion is ≤ 40 mol %). The non-reacted *-COOH* groups may cause undesired types of polymer-LC interaction. New approaches are needed to increase concentration of photosensitive fragments in these polymers.

Synthesis examples

Synthesis of monomer 11. In the solution of 54.5 g (0.5 mol) of 4-aminophenole in 250 ml of dry tetrahydrofuran 50.5 g (1 mol) of triethylamine was added. Then 104.5 g (1.1 mol) of methacryloylchloride was added dropwise to the solution at room temperature with stirring and permanent cooling. The reaction mixture was kept 3 days at room temperature and then poured into 1 l of distilled water. The obtained residue was filtered off and washed with water till neutral reaction in litmus. Crystallization in toluene mixture with silica gel gave 70.3 g of monomer **11** (m.p.=103°-105° C, yield 70.3 wt. %). ^1H NMR identification (400 MHz, CDCl_3), ppm: 7.73 (d, 2H, Ar), 7.0 (d, 2H, Ar), 6.34 (s, 1H, =CH₂), 5.78 (m, 2H, =CH₂), 5.47 (s, 1H, =CH₂), 2.06 (s, 6H, CH₃). UV spectrum (ethanol, $c = 5 \times 10^{-5}$ mol/l): $\lambda_{\text{max}} = 260$ nm, $\epsilon_{\text{max}} = 1.15 \times 10^4$ (l/molxcm).

Synthesis of polymer poly-11. 1.4 g of monomer **11** and 0.014 g of AIBN were dissolved in 17 ml of DMF. The reaction vessel with the solution was subsequently closed air-tight and heated to 80° C for 35 minutes. Thereafter, the reaction vessel was opened and the solution was added dropwise to 150 ml of ethanol while stirring at room temperature. The separated polymer was filtered off, dried, dissolved in 10 ml of DMF, and this solution was added dropwise to 50 ml of ethanol. Filtration and drying at 40°C in a vacuum gave 0.323 g (23 wt. %) of **poly-11**. GPC (PS standard, DMF as mobile phase): $M_n = 28\ 600$, $M_w = 50\ 500$, $M_w/M_n = 1.8$.

Synthesis of copolymer-1. 0.91 g (0.004 mol) of monomer **11** and 1g of 2,2,3,3-tetrafluoropropylmethacrylate (0.004 mol) with 0.0191 g of AIBN were dissolved in 24 ml of DMF. The reaction vessel with the solution was subsequently closed air-tight and solution was heated to 80°C for 40 minutes. Thereafter, the reaction vessel was opened and the solution was added dropwise to 200 ml of diethyl ether. Filtration gave 0.24 g (12 wt. %) of **copolymer 1**. IR identification (KBr), cm^{-1} : broad 3392 (NH), 1752 (-O-CO-), 1668 (amide I), 1508, 1253, 965, 904, 664 (aryl), other signals 2937,1408, 1392, 1170, 1156, 1128, 1016, 805, 712.

Synthesis of polymer P1. 1 g (0.012 mol) of poly(methacrylic acid) in 5 ml of DMF was stirred during 24 hours. To the resulting solution were added 2.12 g (0.012 mol) of 4-methacryloylamino phenole, 2.47 g (0.012 mol) of DCC and 0.49 g of DMAP. This mixture was stirred at 20°C during 5 days, then filtered off and poured into isopropanol. The obtained residue was isolated by filtration and dried in vacuum, giving 0.8 g (28 wt. %) of polymer **P1**. GPC (PS standard, DMF as mobile phase): $M_n = 54\ 000$, $M_w = 86\ 300$, $M_w/M_n = 1.6$.

6.2. Photochemistry: UV/Vis and IR spectroscopy studies

The polymers of this series demonstrate similar changes under UV irradiation. As an example, Fig. 12 presents spectra of **P1** in THF solution (a) and film (b) before irradiation and after successive steps of irradiation. It is seen that the spectra of these polymers contain only one intensive band with a maximum at 240-265 nm. This band is caused by π - conjugated side chain containing various double bonds, such as $C=C$ (aromatic rings and terminal methacryloyl groups) and $C=O$ (carbonyl groups).

According to Fig. 12, the photoinduced spectral changes are similar for solution and film. UV irradiation leads to a gradual decay of the main absorption band and, simultaneously, the growth of the broad band in the long-wave region (300-360 nm). The former change is caused by reduction of

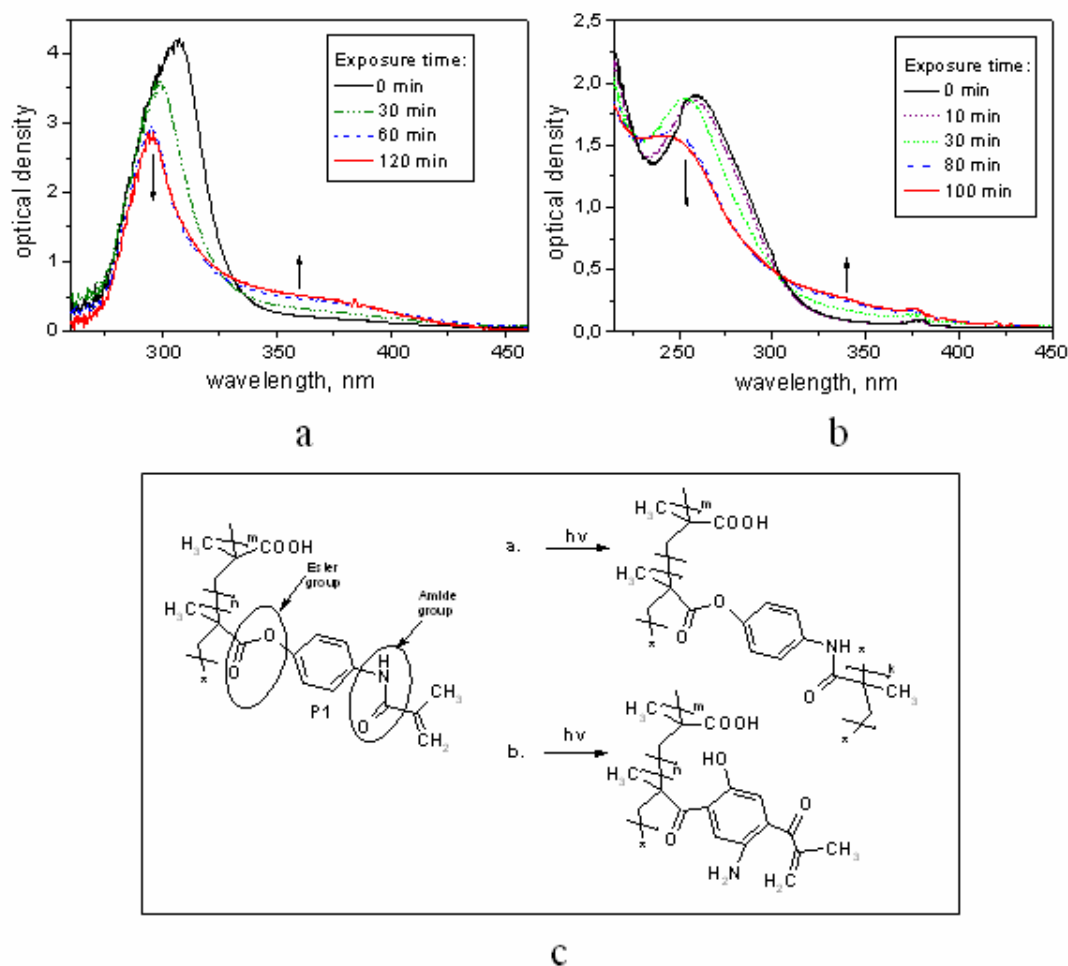


Figure 12. UV/Vis spectra of **P1** in (a) THF solution and (b) film for a sequence of exposure times at light intensity 80 mW/cm². (c) Photochemical transformations of polymer molecules. The upper and lower products are formed in result of photo-polymerization and photo-Fries rearrangements, respectively.

π -conjugation in the molecule and can be caused by saturation of C=C bonds in *NH*-methacryloyl groups and Fries rearrangements. The latter change is typical for Fries rearrangements.

Detecting changes typical for Fries photoreaction, UV/Vis spectra are unable to distinguish different Fries transformations. As demonstrated in Fig. 12 (c), two types of Fries rearrangements, in arylester *Ph-O-CO* and arylamide *Ph-NH-CO* groups, are possible in **P1**. Moreover, because of complexity of polymer structure, UV/Vis spectroscopy cannot unambiguously confirm the polymerization of *NH*-methacryloyl groups. To verify realization of each of these possible reactions, several auxiliary compounds were synthesized. These compounds had simplified structure so

Table 4. Peak positions of IR absorption bands related to photosensitive groups of **P1** [70].

Structural element	Peak position, cm ⁻¹		Assignment
	Experimental	Ref. [68,69]	
Ar-NH-C=O	1668	1680-1630	Amide I, ν (C=O)
	1528	1570-1515	Amide II, ν (C-N)+ δ (C-N-H)
	1322	1330-1200	Amide III, δ (NH)+ δ (OCN)
Ar-O-C=O	1750	1750-1735	ν (C=O)
	1196 and 1166	1200 and 1150-1100	ν (COC)
C=CH ₂	1628	1680-1620	ν (C=C)
	930	930-945	δ (C-H)

that some types of photochemical transformations possible for **P1** were excluded [63]. These studies showed that all three reactions theoretically predicted for **P1** are actually realized under irradiation.

This conclusion was also supported by IR studies. First of all, we identified vibration bands corresponding to arylester, arylamide and methacryloyl groups assuming that these bands are sensitive to the above discussed reactions (Table 4). For the majority of these bands we observed changes after UV irradiation that gave clear evidence for all three photochemical reactions theoretically possible in this polymer [70].

6.3. Photoinduced ordering in polymer films

The photoinduced orientational ordering in polymer films under irradiation with polarized light was studied by polarization UV/Vis spectroscopy and null ellipsometry [63]. For illustration, Fig. 13 presents the data obtained by polarization spectroscopy for **P1**. It can be seen that under irradiation the initially isotropic angular distribution of light absorption is transformed to the anisotropic one with the absorption maximum in the direction perpendicular to the direction of light polarization \mathbf{E} (D_{\perp} absorption coefficient) and the absorption minimum in the \mathbf{E} direction ($D_{//}$). This implies that after irradiation the photoinduced fragments are orientationally ordered in the direction perpendicular to light polarization. Seemingly, due to anisotropic interaction with these fragments, LC molecules are aligned in the same direction. According to Fig. 13 (b), the photoinduced ordering demonstrates saturation trend. Assuming uniaxial ordering in the saturation, the order parameter of photosensitive polymer chains can be calculated

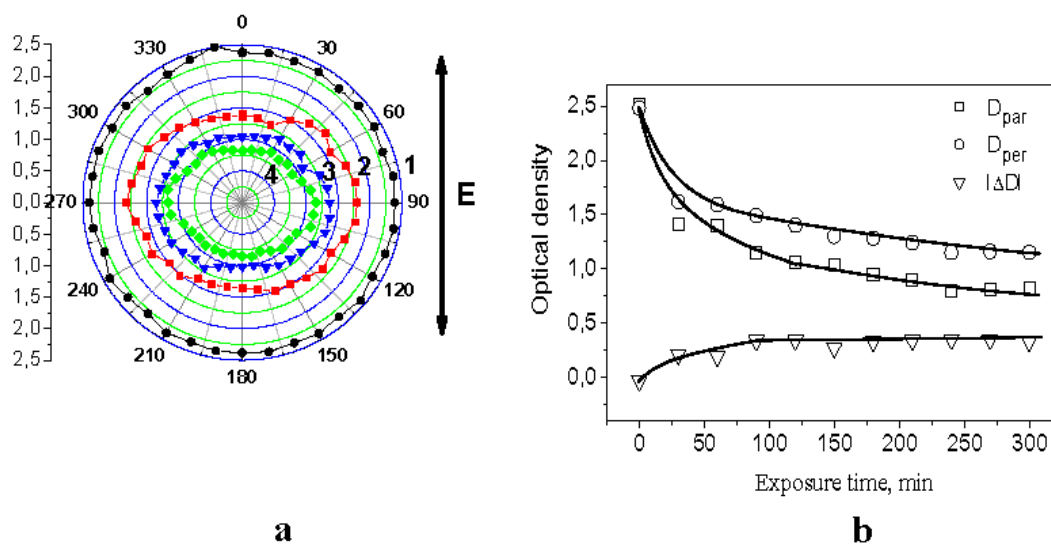


Figure 13. (a) Angular dependence of the optical absorption of the film of **P1** at 265 nm, maximum of the main absorption band, for exposure times 0, 30, 180, 300 min (curves 1, 2, 3 and 4, respectively). **E** marks direction of polarization of exciting light. (b) Optical densities $D_{//,\perp}$ and dichroism $\Delta D = D_{\perp} - D_{//}$ as functions of exposure time for the film of **P1**. $I = 45 \text{ mW/cm}^2$ (modified of ref. [63]).

as $S = (D_{\perp} - D_{//}) / (D_{\perp} + 2D_{//})$. The obtained value is $S \approx 0.11$. The changes in the coefficients of optical absorption under irradiation correspond to angular photoselection mechanism [20-22]. The photoordering features for other polymers of this series are rather similar to those of **P1**.

6.4. LC alignment

The quality of LC alignment with these polymers is strongly dependant on polymerization yield. At high yields (usually, higher than 70 wt. %) the polymer products are highly crosslinked and so insoluble in organic solvents used for film coating purpose. At lower yields (typically, 40-70 wt. %) the materials can be dissolved, but quality of LC alignment is rather poor. Finally, if the yield is lower than some critical value, acceptable LC alignment is detected. The critical values of polymerization yield for these polymers are presented in Table 5. One can see, that the highest yield is obtained for naphthalene containing polymers ($R_5 = 1,4\text{-Nph}$, $1,5\text{-Nph}$). However, these polymers give somewhat worse alignment then the homologues with phenyl core ($R_5 = 1,4\text{-Ph}$, $1,4\text{-OPh}$, $1,4\text{-NHPh}$ and $1,4\text{-COOPh}$). This may be due to the lower shape anisotropy of photosensitive fragments. Finally, the alkyl tail between *O* or *NH* methacryloyl

Table 5. Polymerization yield, solubility and characteristics of LC ZLI2293 alignment for poly(methacrylamidoaryl methacrylates).

Aromatic core, R ₅	Yield, wt. %	Solubility	Alignment grade	LC pretilt angle
1,4-Ph	35	DMF	excellent	0.4°-1.2°
1,4-Nph	48	DMF	good/excellent	0.3°-0.8°
1,5-Nph	50	DMF	good	0°-0.6°
1,4-OPh	29	DMF	excellent	0°-0.5°
1,4-NHPh	30	DMF	excellent /good	1.0°-2.2°
1,4-COOPh	30	DMF	excellent	0°-0.8°

group and aromatic core (monomers with R₅= *1,4-OPh*, *1,4-NHPh*) slightly reduces yield of soluble polymer, but gives rise to some enhancement of LC pretilt angle.

Even below the critical yield, the quality of LC alignment decreases with the yield. As was noted in the synthesis section 6.1, the polymers obtained by way of monomer polymerization have bimodal distribution of molecular weight. The relative content of the latter fraction increases with the polymerization yield and, simultaneously, the quality of LC alignment decreases (Table 3). Thus, perhaps, the low molecular weight fraction plays an essential destructive role in LC alignment.

For the polymers synthesized by polymer analogue reaction we obtained rather encouraging result: these polymers provide high-quality alignment at even rather low degree of attachment of photosensitive fragments. The increase of this parameter above 10 mol % mainly accelerates generation of photoalignment and modifies pretilt angle, but does not significantly affect azimuthal anchoring. This gives us hope that the industrial demands can be met at even low concentration of photosensitive fragments.

For both types of polymers, synthesis conditions can be optimized for the LC alignment of excellent quality. For illustration, Fig. 14 (a) demonstrates alignment in the cell based on **poly-11**. One can judge the high quality of alignment in the areas with parallel and twisted director configuration. Fig. 14 (b) shows that LC uniformly switches in an electric field. The azimuthal anchoring energy grows and saturates with an exposure dose approaching 10⁻⁴ J/m² in the saturation state. This is one of the best results claimed for photoaligning materials.

The pretilt angle for homopolymers was lower than 1.5°. However, it can be dramatically increased by copolymerization of the monomers **11-16** with the monomers containing hydrophobic chains. Figs. 14 (d)-(f) demonstrate properties of the films based on **11-MF-2** series of copolymers. The increase

in the concentration of **MF-2** in the copolymer leads to an increase of its hydrophobicity. This, in turn, results in an increase in pretilt angle. As there is obvious from Fig. 14 (f), full range controlling of pretilt angle can be realized.

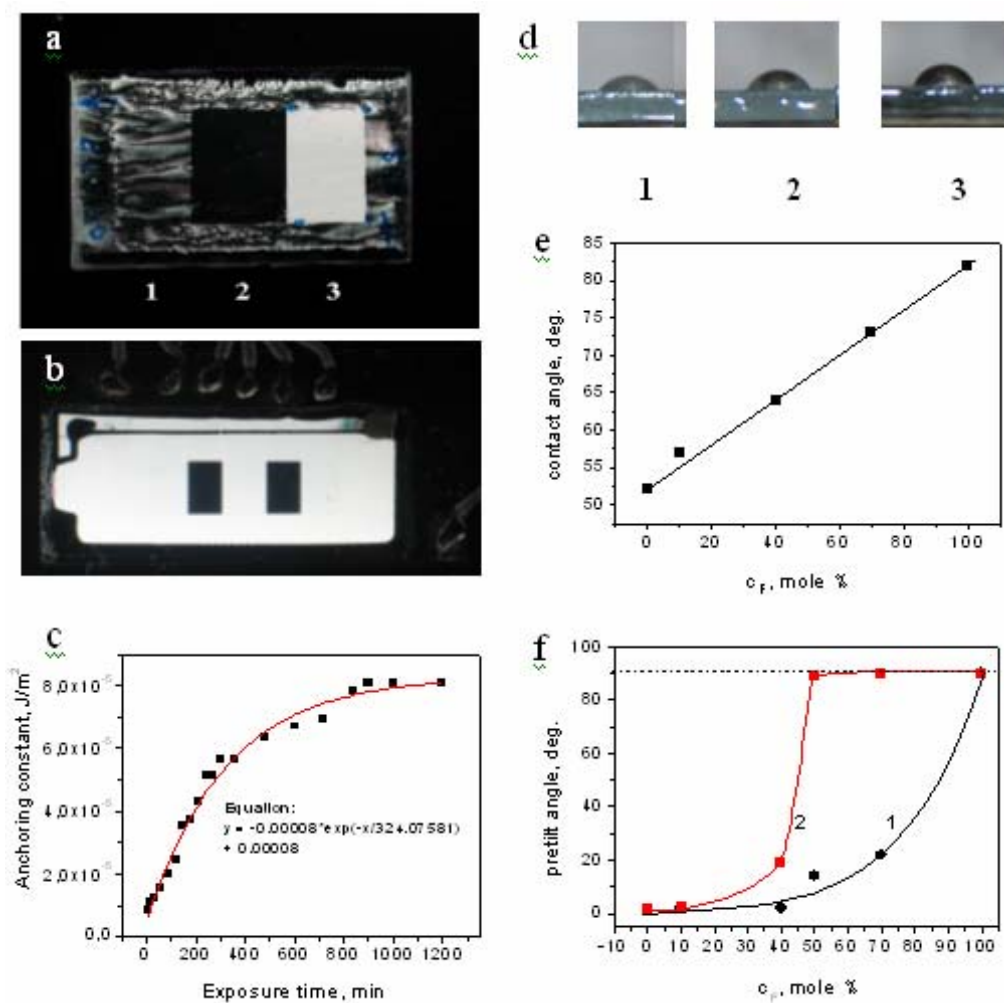


Figure 14. (a, b) Photographs of symmetric LC cells based on **poly-11** photoaligning layers viewed between crossed polarizers. (a) The cell with different types of alignment; marks 1, 2 and 3 designate areas with no alignment, antiparallel and 90° twist alignment. (b) The pixelized cell with 90° twist alignment; black rectangular areas correspond to pixels being under voltage. (c) Azimuthal anchoring coefficient as a function of exposure time for the cell based on **poly-11** photoaligning layers. (d-f) Figures representing properties of the films of copolymers based on monomer **11** and 2,2,3,3,4,4,5,5-octafluoropentyl-methacrylate (**MF-2**). (d) Photos of water drops corresponding to 0, 40 and 100 mol % of **MF-2**, in case 1, 2 and 3, respectively. (e) Water contact angle as a function of concentration of **MF-2** in the copolymer. (f) Pretilt angle vs. **MF-2** concentration curves; 1 – LC MJ961180, 2 – LC ZLI 2293.

LC photoalignment on these polymers is extremely photo- and thermally stable. The high intensity ($I \sim 1 \text{ W/cm}^2$) UV light exposure for 10 hours did not lead to any noticeable destruction of LC alignment. In the temperature tests, the alignment withstand heat 120°C for 5 hours.

The set of these properties makes polymers of this series rather promising for practical applications. However, to evaluate potential of these materials for industrial use, wide range of additional tests should be held, aimed at estimation of LC alignment stability, polar anchoring, parameters of electro-optic response, dielectric properties (*e.g.*, VHR and RDC characteristics), *etc.* Together with our industrial partners we are currently conducting these studies.

7. Conclusion

In summary, we have proposed new strategy in development of photoaligning polymers with reactive $C=C$ bonds. In contrast to widely used $C=C$ groups capable of [2+2] cycloaddition, our materials contain $C=C$ groups capable of polymerization. Due to angularly selective photo-crosslinking of these groups under polarized light, these materials acquire photoaligning function. The photoalignment effect is essentially enhanced if, in parallel with photo-crosslinking, polymer structure allows for one or several photo-Fries rearrangements. Based on this concept, several classes of efficient photoaligning materials have been developed with the culmination in a class of polyarylmethacrylates containing non-polymerized methacryloyl groups.

These polymers require simple synthesis procedure and low cost starting compounds. They have structures quite flexible for design. Due to position of the main absorption band in shortwave UV range and high crosslinking degree, these materials provide alignment of outstanding photo- and thermal stability. The azimuthal anchoring energy on these polymers approaches 10^{-4} J/m^2 , which is claimed for the best photoaligning polymers. The LC pretilt angle can be widely varied by introduction of hydrophobic chains in the polymer structure.

These properties make the described polymers rather attractive for industrial application. The industrial tests are in progress. The problems needed to be solved are better optimization of molecular structures and synthesis ways, use of appropriate UV sources (with emission spectrum in a shortwave UV range), finding of optimal exposure procedure.

Finally, it is worth noting that the idea of combining in a single side-chain of several photosensitive groups, one of which is capable of crosslinking has been very productive. Recently, we found a dramatic improvement in thermal stability of LC alignment on azopolymer films with

introduction in the side azobenzene chains of terminal groups capable of polymerization [71]. Crosslinking of these groups prevent orientational disordering of azobenzene fragments at elevated temperatures and thus stabilize LC alignment. We are confident that the same approach can be productively used to improve the LC alignment properties of other classes of photoaligning materials.

References

1. Takatoh, K., Hasegawa, M., Koden, M., Itoh, N., Hasegawa, R., and Sakamoto, M., 2005, *Alignment Technologies and Applications of Liquid Crystal Devices*, Taylor & Francis.
2. Ichimura, K., Suzuki, Y., Seki, T., Hosoki, A., and Aoki, K., 1988, *Langmuir*, 4, 1214.
3. Dyadyusha, A., Marusii, T., Reshetnyak, V., Reznikov, Y., and Khizhnyak, A. 1992, *JETP Lett.* 56, 17.
4. Schadt, M., Schmitt, K., Kozinkov, V., and Chigrinov, V. 1992, *Jpn. J. Appl. Phys.*, Part 1, 31, 2155.
5. Shannon, P., Gibbons, W., and Sun, S. 1994, *Nature* (London), 368, 532.
6. Hasegawa, M. 2000, *Jpn. J. Appl. Phys.*, 39, Part 1, No. 3A, 1272.
7. Yokoyama, H. and Kimura, M. 2005, *IDW/AD '05*, 49.
8. Yaroshchuk, O., Kyrychenko, V., Tao, D., Chigrinov, V., Kwok, H.S., Hasebe, H., and Takatsu, H. 2009, *Appl. Phys. Lett.*, 95, 021902.
9. Chigrinov, V., Kozinkov, V., and Kwok, H.S. 2008, *Photoalignment of Liquid Crystal Materials: Physics and Application*, Wiley-SID series, UK.
10. O'Neill, M., and Kelly, S. 2000, *J. Phys. D: Appl. Phys.*, 33, R67.
11. Ichimura, K. 2000, *Chem. Rev.*, 100, 1847.
12. Hasegawa, M., and Taira, Y. 1995, *Proc. 21st JLCC*, 344.
13. Yaroshchuk, O., Tereshchenko, A., Lindau, Ju., and Boehme, A. 1996, *SPIE*, 2795, 71.
14. Schadt, M., Seiberle, H., and Schuster, A. 1996, *Nature*, 351, 212.
15. Reznikov, Yu., Yaroshchuk, O., Gerus, I., Homuth, A., Pelzl, G., and Weissflog, W. 1998, *Mol. Materials*, 9, 333.
16. Obi, M., Morino, S., and Ichimura, K. 1999, *Chem. Mater.*, 11, 656.
17. Kawatsuki, N., Hamano, K., Ono, H., Ssaki, T., and Goto, K. 2007, *Jpn. J. Appl. Phys.*, 46 (1), 339.
18. US Patent 6,226,066 (2001).
19. Dyadusha, A., Khizhnyak, A., Marusii, T., Reznikov, Y., Yaroshchuk, O., Reshetnyak, V., Park, W., Kwon, S., Shin, H., and Kang, D. 1995, *Mol. Cryst. Liq. Cryst.*, 263, 399.
20. Dumont, M., and Sekkat, Z. 1992, *Proc. SPIE*, 1774, 188.
21. Yaroshchuk, O., Dumont, M., Zakrevskyy, Y., Bidna, T., and Lindau, J. 2004, *J. Phys. Chem. B*, 108, 4647.

22. Yaroshchuk, O., Kiselev, A., Zakrevskyy, Yu., Bidna, T., Kelly, J., Chien, L.-C. and Lindau, J. 2003, *Phys. Rev. E*, 68, 011803.
23. Pedersen, T., Johansen, P., Holme, N., Ramanujam, P., and Hvilsted, S. 1998, *J. Opt. Soc. Am. B: Opt. Phys.*, 15, 1120.
24. Yaroshchuk, O., Reshetnyak, V., Tereshchenko, G., and Lindau, J. 1999, *Mater. Sci. Eng., C*, 8–9, 211.
25. Weigert, F., 1919, *Verh. Phys. Ges.*, 21, 485; 1921, *Z. Phys.* 5, 410.
26. Yaroshchuk, O., Zakrevskyy, Yu., Kumar, S., Kelly, J., Chien, L.-C., and Lindau, J. 2004, *Phys. Rev. E*, 69 (1), 011702.
27. Yaroshchuk, O., Chigrinov, V., Nadtocha, O., and Kwok, H. 2006, *Liq. Crystals*, 33 (2), 149.
28. Usami, K., Sakamoto, K., Uehara, Y., and Ushioda, S. 2005, *Appl. Phys. Lett.*, 86, 211906.
29. Kumar S., Kim, J.H. and Shi, Y. 2005, *Phys. Rev. Lett.*, 94, 077803.
30. Yaroshchuk, O., Agra, D.M.G., Zakrevskyy, Y., Chien, L.-C., Lindau, J., and Kumar, S. 2001, *Liq. Crystals*, 28, (5), 703.
31. Chigrinov, V., Prudnikova, E., Kozenkov, V., Kwok, H. S., Akiyama, H., Kawara, T., Takada, H., and Takatsu, H. 2002, *Liq. Cryst.*, 29, 1321.
32. West, J., Wang, X., Ji, Y., Kelly, J. R., 1995, *SID 95 Digest*, XXVI, 703.
33. Yaroshchuk, O., and Kadashchuk, A. 2000, *Appl. Surf. Sci.*, 158 (3–4), 357.
34. Hasegawa, M., 1999, *Jpn. J. Appl. Phys.*, 38, L255.
35. Jackson, P. R., and O'Neill, M. 2001, *Chem. Mater.*, 13, 694.
36. Makita, Y., Natsui, T., Kimura, S., Nakata, S., Kimura, M., Matsuki, Y., and Takeuchi, Y. 1998, *J. Photopolym. Sci. Technol.*, 11, 187.
37. Kawatsuki, N., Tadahiyo, A., Kawakami, Y., and Yamamoto, T. 2000, *Jpn. J. Appl. Phys.*, 39, L5943.
38. US Patent 5,389,698.
39. US Patent 6,919,404 B2.
40. Miyachi, K., Kimura, N., Yamada, Y., Mizushima, S. 2010, *IDW'10*, LCT1-1.
41. Maruyama, K., Hayashi, H., Ono, Y., Nozaki, A., Suzuki, Y., Naitoh, S., and Ikariya, T. 2005, *IDW/AD '05*, 1411.
42. Ichimura, K. 2003, *J. Photochem. & Photobiol. A: Chemistry*, 158, 205.
43. Murai, H., Nakata, T., and Goto, T. 2002, *Liquid Crystals*, 29 (5), 669.
44. Kim, D-H., Park, S-K., Kwon, S.-B., Kurioz, Yu., Reznikov, Yu., Tereshchenko, O., and Gerus, I. 2006, *SID 06 Digest*, 867.
45. Wilderbeer, H., Teunissen, J.-P., Bastiaansen, C., and Broer, D. 2003, *Adv. Mater.*, 15 (12), 985.
46. Hwang, J.-Y., Kang, H.-K., Park, C.-J., Seo, D.-S. 2005, *Mol. Cryst. Liq. Cryst.*, 434, 151.
47. Gvozdozskyy, I., Orlova, T., and Terenetskaya, I. 2005, *Mol. Cryst. Liq. Cryst.*, 430, 199.
48. Park, B., Jung, Y., Choi, H., Hwang, H., Kakimoto, M., and Takezoe, H. 1998, *Jpn. J. Appl. Phys.*, 1, 37, 5663
49. Kim, J. Y., Kim, T. H., Kimura, T., Fukuda, T., and Matsuda, H. 2002, *Optical Materials*, 21, 627.

50. Kang, H., Kang, D., and Lee, J-C. 2009, *Polymer*, 50, 2104.
51. Chigrinov, V., Muravski, A., and Kwok, H. S. 2003, *Phys. Rev. E.*, 68, 061702.
52. Kobsa, H. 1962, *J. Organic Chemistry*, 27 (7), 2293.
53. Anderson, J. C., and Reese, C. B. 1960, *Proc. Chem. Soc.* 1960, June, 217.
54. Frechet, J. and Tessier, T., 1985, *Macromolecules*, 18 (3), 317.
55. Li, S., and Guillet, J. 1977, *Macromolecules*, 10 (4), 840.
56. Merle-Aubry, L., Holden, D., Merle, Y., and Guillet, J. 1980, *Macromolecules*, 13, 1138.
57. Hofler, T., Grieber, T., Gstrein, X., Trimmel, G., Jakopic, G., and Kern, W. 2007, *Polymer*, 48, 1930.
58. Kawatsuki, N., Takatsuka, H., and Yamamoto, T. 2001, *Jpn. J. Appl. Phys.*, 40, L.209.
59. Allen, N. S., 1983, *Polymer Photochemistry*, 3, 167.
60. Syromyatnikov, V., Vretik, L., Yaroshchuk, O., Zakrevskyy, Yu., Kim, T. M., Jo, J. H., Kim, J. Y., and Kim, S. H. 2001, *Mol. Cryst. Liq. Cryst.*, 368, 543.
61. Vretik, L., Syromyatnikov, V., Zagniy, V., Paskal, L., Savchuk, O., Yaroshchuk, O., Dolgov, L., Kyrychenko, V., and Lee, C.-D. 2007, *Mol. Cryst. Liq. Cryst.*, 479, 121.
62. Vretik, L., Paskal, L., Syromyatnikov, V., Zagniy, V., Savchuk, O., Dolgov, L., and Yaroshchuk, O. 2007, *Mol. Cryst. Liq. Cryst.*, 468, 173.
63. Kyrychenko, V., Smolyakov, G., Zagniy, V., Vretik, L., Paskal, L., Syromyatnikov, V., and Yaroshchuk, O. 2008, *Mol. Cryst. Liq. Cryst.*, 496, 278.
64. Vretik, L., Syromyatnikov, V., Zagniy, V., Savchuk, E., and Yaroshchuk, O. 2008, *Mol. Cryst. Liq. Cryst.*, 486, 57.
65. Gryshchuk, L., Vretik, L., Syromyatnikov, V., Novikova O., Paskal P., Voytekunas V., and Abadie M.-J. 2004, *Polymer International*, 53, 27.
66. Gryshchuk, L., Vretik, L., Syromyatnikov, V. 2002, *Materials Science*, 20, 5.
67. Konovalov, V., Muravski, A., and Yakovenko, S. 2000, *SID'00 Digest*, 620.
68. Gunzler, H., Gremlich, H.U. *IR Spectroscopy. An Introduction.* Wiley-VCH: Weinheim, (2002).
69. Bellamy, L.J. *The infra-red spectra of complex molecules.* Wiley: New York, (1963).
70. Vretik, L., Kyrychenko, V., Smolyakov, G., Yaroshchuk, O., Zagniy, V., Gavrilko, T., Syromyatnikov, V. 2011, *Mol. Cryst. Liq. Cryst.*, 536, 224.
71. Kyrychenko, V., Vretik, L., Yaroshchuk, O., Nadtocka, O., Syromyatnikov, V., *Book of abstracts of ILCC'10*, July 12-16, Krakow, Poland, p. 216.